Interaction of optical phonons with a one-component plasma

W. E. Bron and S. Mehta
Department of Physics, University of California, Irvine, California 92717

J. Kuhl
*Max-Planck-Institut für Festkörperforschung, 7000 Stuttgart 80, Federal Republic of Germany**
and Department of Physics, University of California, Irvine, California 92717

M. Klingenstein
Max-Planck-Institut für Festkörperforschung, 7000 Stuttgart 80, Federal Republic of Germany
(Received 7 November 1988; revised manuscript received 23 January 1989)

The effect of a strongly damped, thermally excited, one-component electronic plasma on near-zone-center longitudinal-optical phonons in GaP has been studied in detail. The bandwidths, peak positions, and spectral functions as obtained from incoherent Raman scattering compare very well with the expected dielectric response of a phonon-plasma coupled mode. It is possible to recover, by these means, the dependence of the effective phonon damping rate, the plasma damping rate, and the plasma frequency on the ambient temperature and the carrier concentration.

I. INTRODUCTION

We have previously reported[1,2] a measurement of the dephasing time, T_2, of near-zone-center longitudinal-optical (LO) phonons in high-purity crystalline GaP. It was demonstrated that the temperature dependence of the dephasing time is dominated by three-phonon (anharmonic) interactions for temperatures less than about 150 K. Above this temperature, T_2 was observed to be shorter than that explicable in terms of three phonon interactions. Similar observations, deduced from studies of the temperature dependence of the bandwidths and the peak frequencies of incoherent Raman-scattering lines, have been previously reported in the literature.[3–5] The increased bandwidth (shorter dephasing time) has been variously proposed to stem from the presence of higher-order phonon-phonon interactions,[3] insufficiencies of anharmonic lattice theory,[4] and/or the presence of free carriers from thermally or optically activated donor states.[2,5] The theoretical basis necessary to resolve the roles of these various possible contributions requires the introduction of additional fitting parameters.

We now show for n-doped GaP that the temperature dependence of the bandwidths, peak frequencies, and other parameters of a coupled phonon-plasma system can be accounted for in terms of simple dielectric-response theory without the introduction of fitting parameters. Specifically, we have investigated in some detail the interaction of LO phonons in GaP with a thermally activated (electron) plasma of varying concentration. In principle, our investigation of this system is similar to that reported by Hon and Faust.[6] However, as will be noted below, the treatment of the phonon-plasma coupling, the temperature range of the measurements, plus the experimental results and their analysis, differ considerably.

II. EXPERIMENTAL CONDITIONS AND RESULTS

Before proceeding to the present results, it is worth noting the following factors which influence the experiment.

(a) In the present experiment the observables are the bandwidth, peak height, and spectral line-shape function of the incoherent Raman scattering from the LO-phonon–coupled mode. In our earlier work[1,2] we observed instead the dephasing time of near-zone-center LO phonons by (picosecond) time-resolved coherent anti-Stokes Raman scattering (TRCARS). It can readily be shown, as long as the incoherent Raman-scattering spectral function is Lorentzian and the phonon component of the TRCARS signal decays exponentially, that the bandwidth $\Delta\nu$ and the dephasing time T_2 are simply related by $\Delta\nu(\mathrm{cm}^{-1})=(\pi c T_2)^{-1}$. Thus, either measurement yields $\Delta\nu$ and T_2, so that the choice of the measuring technique need depend only on the experimental conditions (c is the speed of light).

(b) In forward-scattered incoherent Raman processes, or forward-scattered coherent Raman excitation (CRE),[2] only phonons with wave vector of the order 10^2–10^3 cm^{-1} can be excited and detected.

(c) Electronic carriers photoexcited high into the conduction band of GaAs, at densities below 5×10^{16} cm^{-3}, have been shown[7,8] to lose energy by LO-phonon emission through a multiple-step cascade with a time of ~150 fs per cascade step. A time of a few picoseconds is required to form a thermalized electron-hole plasma at some conduction-band minimum. We assume that the temporal factors are essentially the same in GaP as in GaAs. Thus, near zero-center optical phonons observed in the cw incoherent Raman-scattering or in the picosecond time-resolved CARS measurements can be ex-

 ©1989 The American Physical Society

pected to interact only with a plasma of carriers.

(d) GaP differs from GaAs in that GaP is a so-called "indirect-gap" semiconductor, whereas GaAs is a "direct-gap" semiconductor. This refers to the fact that in GaAs photoionization from the maximum of the valence (say at the Γ point) to a minimum in the conduction band can be reached without a change in the carrier wave vector, whereas that is not the case in GaP, which has lowest-lying conduction-band minima at the X point in the band structure.[9] In the present experiment carrier excitation occurs through thermal ionization of donor impurity states in which changes in wave vector do not play a role. Nevertheless, once thermally excited the carriers in GaP will most likely form a plasma at equivalent minima in the band structure near the X point of the Γ_1 band.[9] Such plasmas succumb to carrier-scattering processes[10] which differ from those in, e.g., GaAs, which possesses a single band minimum.[10]

(e) Plasma are damped even in the absence of phonons, the damping arising from, among other factors, carrier-carrier, intervalley, and interband scattering. The plasma damping rate in GaP is known to be high,[6] possibly due to the additional intervalley scattering which may be present in indirect-gap semiconductors. Thus, as a result of phonon-plasma coupling, even modest carrier concentrations in GaP readily cause a decrease in T_2 below the (1–2)-ps limiting temporal resolution of our TRCARS system. This is the basis for choosing incoherent Raman scattering, rather than TRCARS measurements, except for the case of a very pure sample.

Incoherent Raman scattering was carried out in a standard forward-scattering geometry using a cw krypton laser operating at 647.1 nm and a power of 100 mW. Samples of GaP, with n-type doping of various nominal concentrations, were held at ambient temperatures from 5 to 300 K.

The temperature dependence of the Hall coefficient was independently determined for each of the samples of GaP (except sample a). Values for the corresponding temperature dependence of the carrier concentration, $n_c(T)$, for three relatively weakly doped samples are shown in Fig. 1. We chose $n_c(285\ \text{K})$ as a way of identifying the various samples as indicated in Table I. Samples $a-d$ and f were doped with tellurium, whereas sample e was doped with silicon.

Several measurements of the incoherent Raman-scattering intensity were carried out for each sample, and at each ambient temperature, except for the purest sample, for which several TRCARS measurements were performed. Figures 2(a)–2(d) indicate a series of Raman-scattering lines from sample c held at 50, 100, 175, and 250 K. The solid circles represent a subset of all data points taken and the solid lines are Lorentzian spectral distributions fitted to the observed peak frequencies and bandwidth [full width at half maximum (FWHM)].[11] Similar Lorentzian line profiles are obtained for all other samples and temperatures.

The open triangles in Figures 3–5 are a compilation of observed peak frequencies of the "phononlike" coupled mode ω_+, and the observed effective damping rates of the LO-phonon–coupled mode for various ambient temperatures. In general, the effective damping rate Γ_{eff} for any one sample increases with temperature, whereas ω_+ increases or decreases depending on the doping levels. For any one temperature, both Γ_{eff} and ω_+ increase with the doping level.

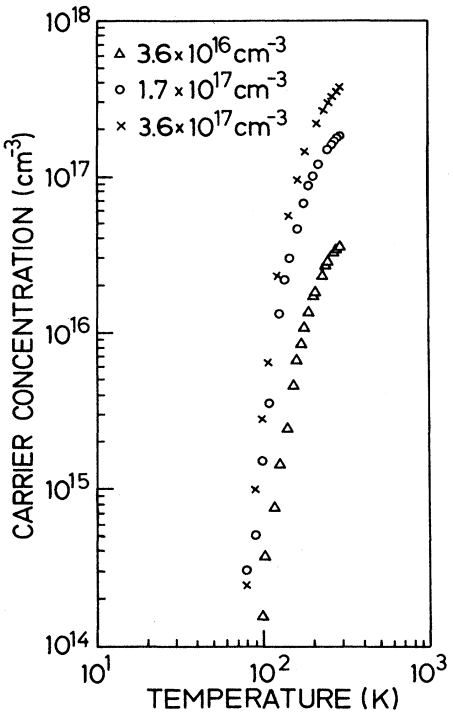

FIG. 1. Carrier concentration as function of ambient temperature as obtained from Hall-coefficient measurements for sample b, open triangles; sample c, open circles; sample d crosses.

III. THEORY AND ANALYSIS OF RESULTS

We treat the coupled phonon-plasma system in terms of a dielectric response function, $\epsilon(\omega)$, given by

$$\epsilon(\omega)=\epsilon_\infty+\frac{\Omega^2}{\omega_T^2-\omega^2-i\omega\Gamma}-\frac{\omega_p^2}{\omega(\omega+i\gamma)}\ . \tag{1}$$

In Eq. (1), $\Omega^2=\epsilon_\infty(\omega_L^2-\omega_T^2)$, ω_L is the LO-phonon fre-

TABLE I. Identity of samples and effective masses of carriers.

Sample	Concentration at 285 K (cm^{-3})	m^*/m_e
a	$<1.5\times10^{16}$	
b	3.6×10^{16}	0.35
c	1.7×10^{17}	0.35
d	3.6×10^{17}	0.37
e	1.3×10^{18}	0.57
f	1.8×10^{18}	0.56

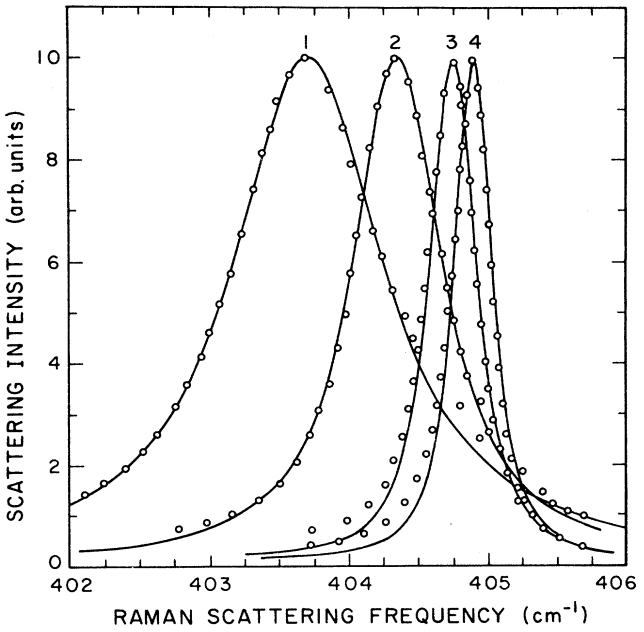

FIG. 2. Observed incoherent Raman scattering lines from sample c held at an ambient temperature of 1, 250 L; 2, 175 K; 3, 100 K; 4, 50 K (also see Ref. 11).

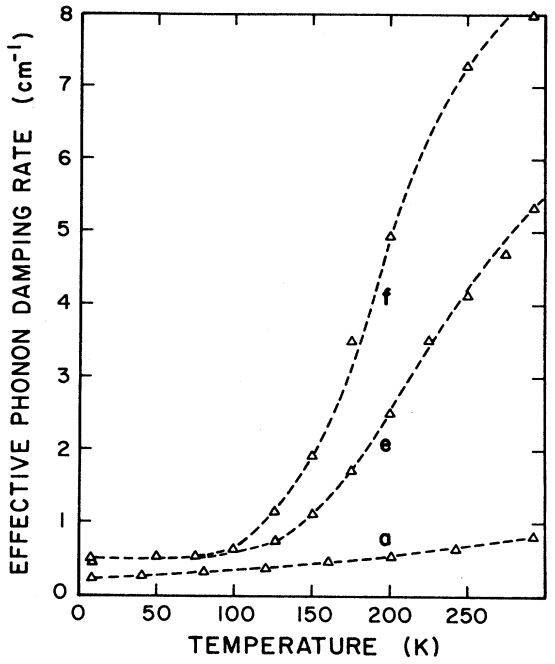

FIG. 4. Compilation of the effective damping rate of the LO-phonon–plasma–coupled mode for the pure sample (a) and two nominally heavily doped samples (e and f).

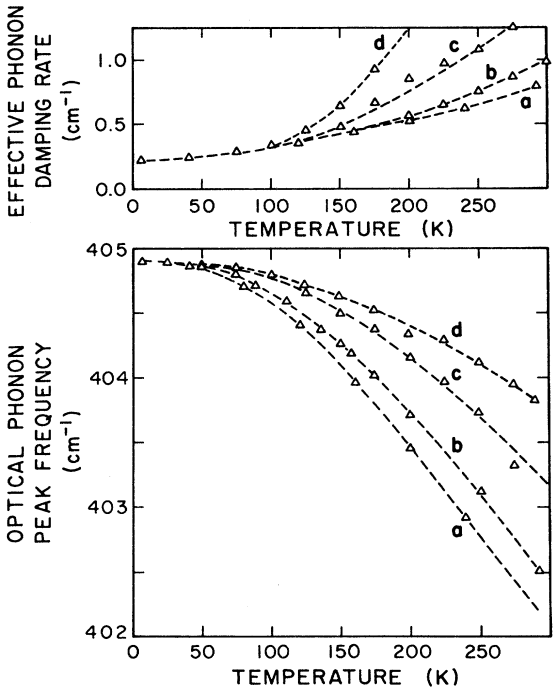

FIG. 3. Lower graph: compilation of observation peak frequencies, ω_+ (open triangles), associated with the LO-phonon–coupled mode as a function of ambient temperature. Results for samples a–d are as marked in the figure. Upper graph: compilation of the effective damping rate of the LO-phonon–coupled mode for samples a–d.

quency, ω_T is the transverse-optical- (TO-) phonon frequency, Γ is the damping rate of the LO phonons in the absence of the plasma, γ is the damping rate of the plasma in the absence of the phonons, $\omega_p^2=\epsilon_\infty\tilde{\omega}_p^2$, ϵ_∞ is the

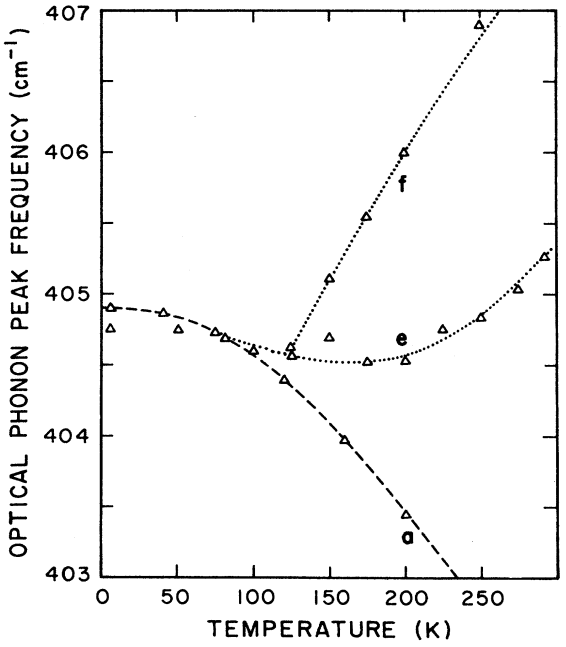

FIG. 5. Compilation of the peak frequency of the LO-phonon–plasma–coupled mode for the purest sample (a) and two nominally heavily doped samples (e and f).

static dielectric constant in the presence of the ion-core background, and $\tilde{\omega}_p$ is the plasma frequency in the presence of the ion-core background.

The real part of $\epsilon(\omega)$ set equal to zero leads to the eigenfrequencies of the coupled modes and the imaginary part of $1/\epsilon(\omega)$ leads to a spectral function, $S(\omega)$, analogous to the structure factor of nuclear scattering. In the past, various parameters of Eq. (1) have been neglected. Thus, either γ and/or Γ are not taken into account depending on their relative magnitude. We have obtained instead a rigorous solution of Eq. (1) which contains γ and Γ_{eff} with the only requirements that Γ_{eff} (~ 5 cm^{-1}) $\ll \omega_+$ (~ 400 cm^{-1}) and that $\omega \approx \omega_L$ [i.e., that $\epsilon(\omega)$ is evaluated only in the neighborhood of the peak of the LO-phonon–coupled mode]. The solutions to Eq. (1), with these restrictions, are

$$\omega_{\pm}^2 = \tfrac{1}{2}(\omega_L^2 + \tilde{\omega}_p^2 - \gamma^2) \pm \tfrac{1}{2}[(\omega_L^2 + \tilde{\omega}_p^2 - \gamma^2)^2 + 4(\omega_L^2\gamma^2 + \tilde{\omega}_p^2\gamma\Gamma - \tilde{\omega}_p^2\omega_T^2)]^{1/2} \quad (2)$$

and

$$S(\omega) = \frac{\Omega^2(\omega_L^2+\gamma^2)}{\epsilon_\infty^2(\omega_L^2-\gamma^2-\tilde{\omega}_p^2)} \frac{1}{4\omega_+} \left[\frac{\Gamma_{\text{eff}}}{(\omega_+-\omega)^2+(\Gamma_{\text{eff}}/2)^2} \right] . \quad (3)$$

Here,

$$\Gamma_{\text{eff}} \equiv \Gamma + \left[\frac{\tilde{\omega}_p^2\Omega^2\gamma}{(\omega_L^2+\gamma^2-\tilde{\omega}_p^2)\omega_L^2\epsilon_\infty} \right] \quad (4)$$

where Γ_{eff} is the effective damping rate of the LO-phonon–coupled mode in the presence of the plasma. Here, ω_- stands for the "plasmalike" coupled mode. Note from Eq. (3) that the predicted spectral function, $S(\omega)$, has a Lorentzian shape as, indeed, observed experimentally (see, e.g., Fig. 1 and Ref. 9).

Thus, there are two equations, the ω_+ component of (2) and (4), for the two unknown quantities $\tilde{\omega}_p$ and γ. Γ is obtained from the previously reported TRCARS measurements on sample *a*, i.e., on the very-high-purity sample of GaP. In what follows it is assumed that in the "pure" sample the effect of thermally activated carriers is negligibly small. Thus, the curves marked *a* in Figs. 3–5 represent the effects on $\Gamma(T)$ and $\omega_L(T)$ solely due to thermal expansion of the lattice and anharmonic dephasing of the LO phonons.[2] Thus, deviation from the parameters which describe the pure sample imply the additional interaction with the thermally activated one-component plasma.

Exact solutions of Eqs. (2) and (4) for $\tilde{\omega}_p$ and γ as a function of temperature are obtained through an iterative process which starts with an approximate value of γ and ends when stable values of $\tilde{\omega}_p$ and γ are found. The corresponding values are displayed in Figs. 6 and 7. It follows from summing ω_+^2 and ω_-^2 of Eq. (2) that $\omega_-^2 = \tilde{\omega}_p^2 - \gamma^2$. We find, for the full range of samples and temperatures, that $\gamma \gtrsim \omega_-$; that is, that the Raman scattering peak at ω_- is either strongly, or as in most cases, overdamped. This accounts for the observation that the scattering peak associated with ω_- is only barely detectable. We do not consider it further.

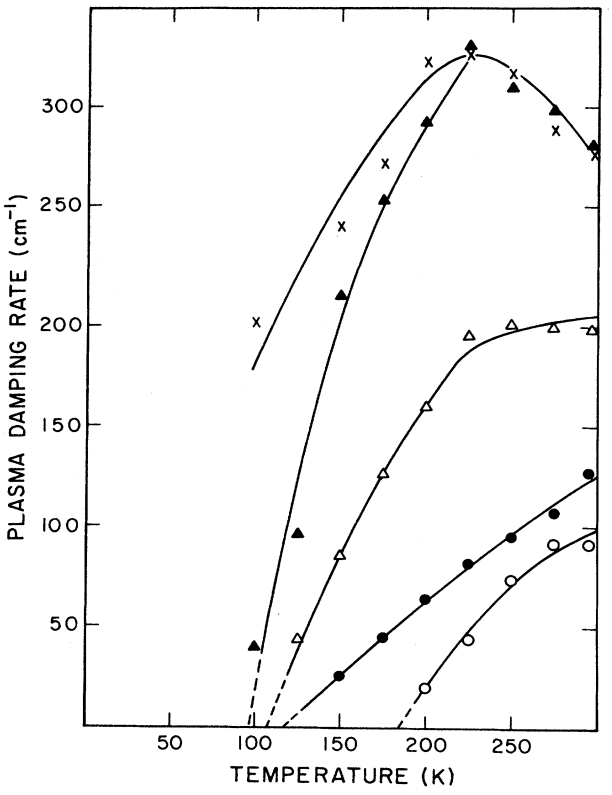

FIG. 6. The plasma damping rate γ as a function of the ambient temperature as obtained through exact solutions of Eqs. (2) and (4). The curves are marked as follows: sample *b*, open circles, sample *c*, solid circles; sample *d*, open triangles; sample *e*, solid triangles; sample *f*, crosses.

Independent measurements of the Hall coefficient for all samples and temperatures (except the pure sample) makes it possible to convert the independent variable from ambient temperatures to carrier concentration, n_c. The results are shown in Figs. 8–11.

It is now possible to make a number of general observations of the behavior of the coupled phonon-plasmon system. First, note that Eqs. (2) and (4) correctly reduce Γ_{eff} to Γ and ω_+ to ω_L as $\tilde{\omega}_p$ goes to zero. This is not the case with the formulation of Hon and Faust. Also note from Figs. 3(a) and 5 and Eq. (2) that deviations from ω_+ relative to ω_L vary roughly as $\tilde{\omega}_p^2 - \gamma^2$. Thus, as the carrier concentration (and $\tilde{\omega}_p^2$) increases, ω_+ increases relative to ω_L, but the plasma damping, γ, tends to reduce this increase. Examination of Eq. (2) further yields, that if $\tilde{\omega}_p = 0$, regardless of the value of γ, $\omega_+ = \omega_L$ and $\Gamma_{\text{eff}} = \Gamma$. In contrast, if $\gamma = 0$, $\Gamma_{\text{eff}} = \Gamma$ and $\omega_+ \geq \omega_L$ depending on whether $\tilde{\omega}_p \geq 0$. Thus if, as in Fig. 3 for $T \lesssim 175$ K, $\Gamma_{\text{eff}} = \Gamma$, but, as in Figs. 3 and 5, $\omega_+ > \omega_L$ it follows that $\gamma = 0$. This accounts for the various ap-

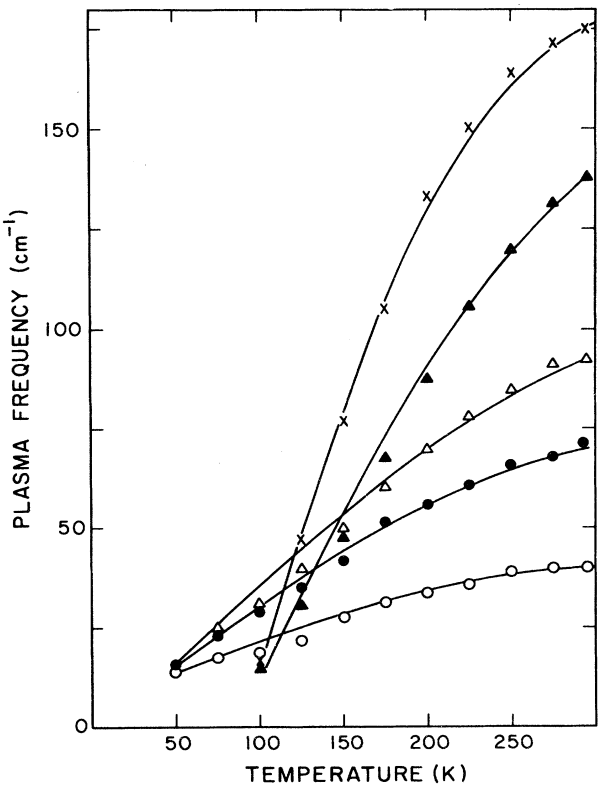

FIG. 7. The plasma frequency $\tilde{\omega}_p$ as a function of the ambient temperature and as obtained through exact solutions of Eqs. (2) and (4). See caption of Fig. 6 for identification of the samples.

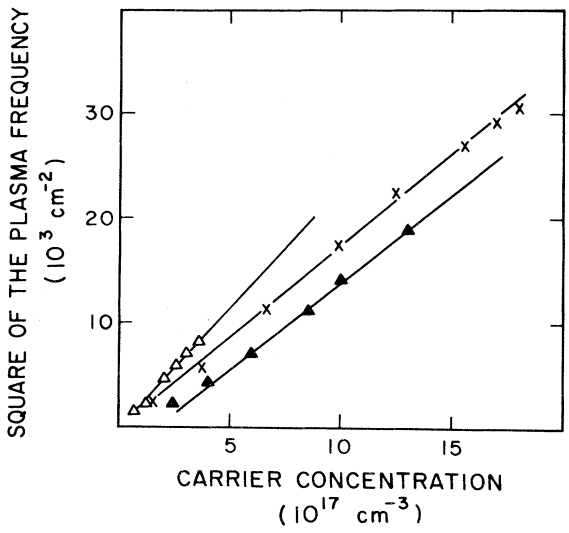

FIG. 9. $\tilde{\omega}_p^2$ as a function of the carrier concentration. Sample *d*, open triangles; sample *e*, solid triangles; sample *f*, crosses.

parent intercepts of $\gamma(T)$ with the temperature axis of Fig. 6.

The accuracy of the measurements of ω_+ and Γ_{eff} (see Figs. 3–5) is not, however, sufficient to rule out the possibility that ω_+ and Γ_{eff} differ, respectively, from ω_L and Γ all the way back to 0 K. If this is the case, then $\gamma(T)$ need not extrapolate to the temperature axis as shown in Fig. 6, but, rather, γ could be greater than zero down to the lowest temperature (or carrier concentration). Therefore, we cannot rule out the possibility that some

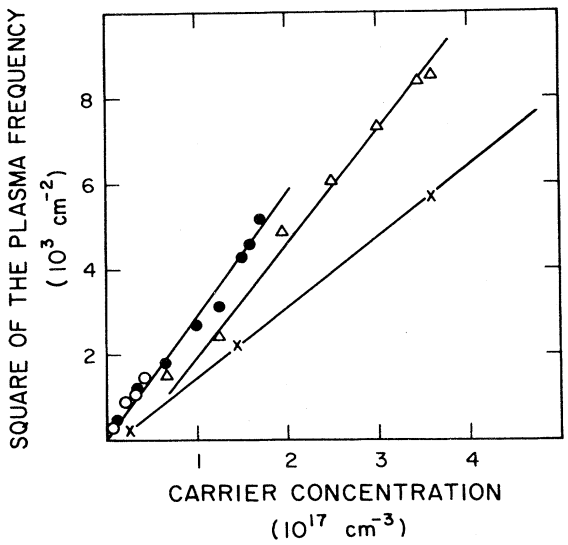

FIG. 8. $\tilde{\omega}_p^2$ as a function of the carrier concentration. Sample *b*, open circles; sample *c*, solid circles; sample *d*, open triangles; sample *f* crosses.

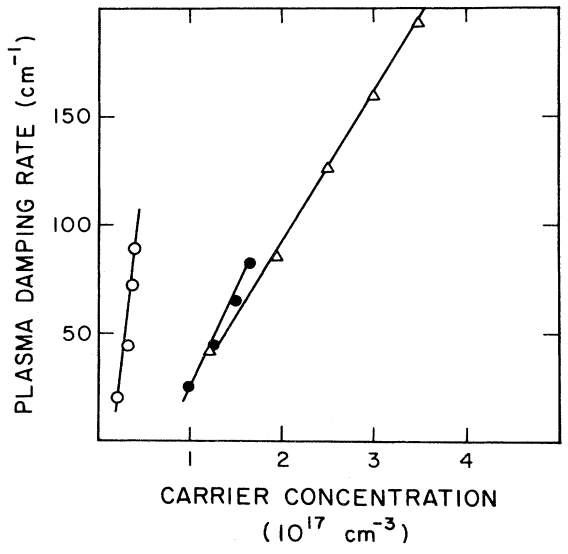

FIG. 10. γ as a function of the carrier concentration. Sample *b*, open circles; sample *c*, solid circles; sample *d*, open triangles.

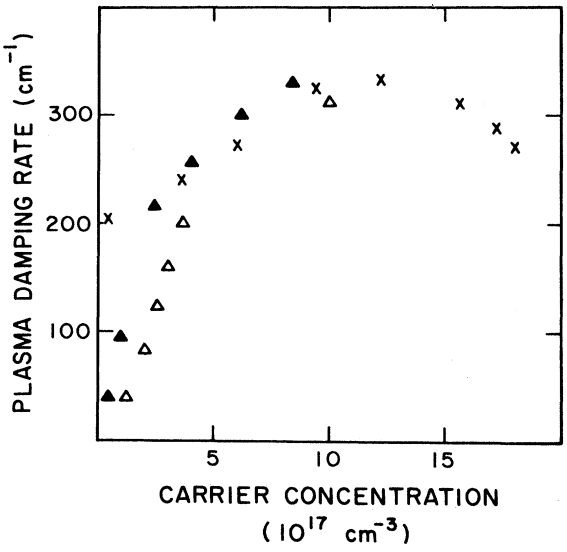

FIG. 11. γ as a function of the carrier concentration. Sample *d*, open triangles; sample *e*, solid triangles; sample *f*, crosses.

temperature- (and therefore carrier-concentration-) independent plasma damping is present in the coupled system, although such effects are not directly observed.

Figure 7 illustrates the expected trend that ω_+ increases with temperature, i.e., with increasing carrier concentration. However, the intercepts with the temperature axis are grouped into two different values depending on whether or not n_c(285 K) is greater than, or less than, $\sim 10^{18}$ cm^{-3}. Sample *e* is doped with silicon, whereas sample *f* is doped with tellerium. Thus, the dopant species is not a likely cause of this observation. On the other hand, higher dopant concentration may cause defect clusters which may have differing ionization energies. However, we have not pursued this point further.

It is also not clear why $\gamma(T)$ saturates, and even eventually decreases, with increasing temperature. Although saturation of $\gamma(T)$ may imply depletion of the donor states, it is difficult to account for the decrease in $\gamma(T)$ and the lack of a corollary effect in $\tilde{\omega}_p$.

The dependence of $\tilde{\omega}_p$ on n_c, as shown in Figs. 8 and 9, can be used to obtain the carrier effective mass, m^*, through the well-known relation $\tilde{\omega}_p^2 = n_c e^2/\epsilon_0 \epsilon_\infty m^*$ in which e is the carrier charge, and ϵ_0 is the static dielectric constant. The results are presented in Table I. This result must be compared to m^* obtained from its components as listed in the literature;[12] namely, $m_\perp = 0.22$, $m_\parallel = 0.87$, and

$$(m^*)^{-1} = \tfrac{2}{3} m_\perp^{-1} + \tfrac{1}{3} m_\parallel^{-1} ,$$

which leads to $m^*/m_e \sim 0.3$. Here again we note that the results for the two heaviest doped samples ($n_c > 10^{18}$ cm^{-3}) differ from those of the lighter doped samples ($n_c < 10^{18}$ cm^{-3}). Whether or not these differences [and those in $\gamma(T)$ and $\gamma(n_c)$] as shown in Figs. 10 and 11 reflect the presence of the well-known "camel's-back structure" in the band structure of GaP at the X point is outside the ability of this experiment to decide.

As a comparison to the present results on $\tilde{\omega}_p$ and n_c, we list in Table II the earlier results of Hon and Faust.[6] The comparison is restricted in a number of ways. For example, only results for room-temperature values are listed since this is the only temperature considered in Ref. 6. Moreover, the independent measurements of the Hall coefficient reported in the present work allow independent experimental determination of $\tilde{\omega}_p$ and n_c. In comparison, Hon and Faust[6] rely on the well-known equation stated at the beginning of their Sec. IV and on an unexplained value of $m^*/m_e = 0.73$ in order to determine values of n_c from the experimental value of $\tilde{\omega}_p$.

IV. DISCUSSION

It is clear that the dielectric response function given by Eq. (1) adequately accounts for the interaction between the damped LO-phonon modes and strongly damped one-component plasma modes. The derivation adopted here for the parameters of the coupled phonon-plasma system represents a straightforward application of dielectric response theory. Furthermore, it avoids the somewhat obscure formulation used by Hon and Faust. Moreover, in the present method, various useful parameters, such as the effective phonon damping rate, the plasma damping rate, the plasma frequency, and the dependence of these parameters on temperature and carrier concentration, can be readily recovered.

We take preliminary note of an apparent difference between phonon-plasma interactions depending on whether a one-component or a two-component plasma is involved. The results of the present investigation clearly demonstrate a strong coupling between the LO phonon and a heavily damped one-component plasma. Thus, the effective damping rate of the phonon-coupled mode is continuously increased as the plasma concentration increases. Because the plasma is strongly damped the scattering at ω_- is barely observable. In contrast, Kardontchik and Cohen[13] report no observable damping in an undoped GaP sample subjected to photoexcitation of a two-component (electron-hole) plasma varying in concentration from 0.5×10^{18} to 5×10^{18} cm^{-3}. In this case, however, the lack of any observable damping of the cou-

TABLE II. Carrier concentration and plasma frequency.

Hon and Faust (Ref. 6)		Present work	
Carrier conc. $10^{-17} n_c$ (cm^{-3}) (at room temp.)	Plasma freq. $\tilde{\omega}_p$ (cm^{-1})	Carrier conc. $10^{-17} n_c$ (cm^{-3}) (at 295 K)	Plasma freq. $\tilde{\omega}_p$ (cm^{-1})
2.6	59.4	0.36	38.0
8.2	105.1	1.70	72.3
9.2	111.2	3.60	92.6
12.0	124.3	13.00	138.8
26.0	186.6	18.00	175.8

pled state may be an experimental artifact due to a limiting spectral resolution of ~ 5 meV (40 cm^{-1}),[13] which is a factor of 5 more than the maximum value of the bandwidth of the ω_+ mode reported in the present study. Nevertheless, Kadontchik and Cohen report observation of the full ω_- peak over a range of excitation energies (see Fig. 2 of Ref. 13), whereas we were able to observe only a very wide, overdamped response in the ω_- region in sample *e* near room temperature. A possibly related observation has been reported by Rhee and Bron,[14] who find that the presence of a photoexcited two-component plasma influences the generation of LO phonons in GaP through coherent Raman excitation (CRE). It is observed that the phonon concentration produced by ever increasing laser pump power reaches a maximum, and then actually decreases to zero. Throughout this process the bandwidth of the LO phonons was observed to remain constant, although, again, the spectral resolution (~ 9 cm^{-1}) was poor compared to the broadest bandwidth (~ 8 cm^{-1}) reported in the present work. Taken at face value, this set of observations implies that the damping of LO phonons coupled to a one-component plasma differs from that coupled to a two-component plasma. If this observation is confirmed by more careful experimentation, then the origin of this difference deserves further attention.

Finally, we note that the main conclusion of this investigation remains intact, namely, that the presence of a strongly damped one-component plasma strongly decreases the effective lifetime of the phonon-coupled mode, and that the behavior of the coupled system is explicable in terms of standard dielectric response theory.

ACKNOWLEDGMENTS

One of us (W.E.B.) acknowledges funding through the U.S. National Science Foundation Grant No. DMR-86-03888, and W.E.B. and J.K. acknowledge support through North Atlantic Treaty Organization Grant No. 0034188. W.E.B and S.M. are grateful to Dr. D. Mills for helpful discussions. We also thank the group of Dr. K. Ploog of the Max-Planck-Institut for their help in performing the measurements of the Hall coefficient. We are indebted to N. Stath, Siemens AG (Regensburg) for the Te-doped samples and K. Matsumoto for the Si-doped sample of GaP.

---

*Permanent address.

[1]J. Kuhl and W. E. Bron, Solid State Commun. **49**, 935 (1984).

[2]W. E. Bron, J. Kuhl, and B. K. Rhee, Phys. Rev. **34**, 6961 (1986).

[3]B. K. Bairamov, Yu. E. Kitaev, V. K. Negoduiko, and Z. M. Khashkhozhnev, Fiz. Tverd. Tela (Leningrad) **16**, 2036 (1974) [Sov. Phys.—Solid State **16**, 1323 (1975)].

[4]J. Menendez and M. Cardona, Phys. Rev. B **29**, 2051 (1984).

[5]E. Haro, M. Balkanski, R. F. Wallis, and K. H. Wanser, Phys. Rev. B **34**, 5358 (1986).

[6]D. T. Hon and W. L. Faust, Appl. Phys. **1**, 246 (1973).

[7]D. von der Linde, J. Kuhl, and H. Klingenberg, Phys. Rev. Lett. **44**, 1505 (1980).

[8]J. A. Kash, J. C. Tsang, and T. M. Hvam, Phys. Rev. Lett. **54**, 2151 (1985).

[9]See, e.g., M. L. Cohen and T. K. Bergstresser, Phys. Rev. **141**, 789 (1966).

[10]See, e.g., K. Seeger, *Semiconductor Physics* (Springer, Berlin, 1973).

[11]The relatively narrow line shapes obtained at low temperatures were corrected for Gaussian instrumentational broadening, as well as the laser line shape, using the tables of Posener for Voigt profiles [D. W. Posener, Aust. J. Phys. **12**, 184 (1959)].

[12]*Landolt-Börnstein, Numerical Data and Fundamental Relationships in Science and Technology,* Vol. 17a: *Semiconductors*, edited by K. H. Hellwege (Springer, Berlin, 1982), p. 207.

[13]J. E. Kardontchik and E. Cohen, Phys. Rev. Lett. **42**, 669 (1979).

[14]B. K. Rhee and W. E. Bron, Phys. Rev. B **34**, 7107 (1986).